THE INJECTOR

DOI: 10.5281/zenodo.8021810
The Injector 2023;2(2):68-76

Original Article

Histomorphological and histopathological evaluation of the effects of ovarian hyperstimulation syndrome on kidney, liver and lung in the rats

Filiz Yılmaz[1], Orkun İlgen[2], Sefa Kurt[2], Bayram Yılmaz[3]

[1]Hitit University, Erol Olçok Training and Research Hospital, In Vitro Fertilization Center, Çorum, Turkey
[2]Dokuz Eylül University Faculty of Medicine, Department of Obstetrics and Gynecology, İzmir, Turkey
[3]Hitit University Erol Olçok Training and Research Hospital, Department of Pathology, Çorum, Turkey

Abstract

Objective: Ovarian hyperstimulation syndrome (OHSS) is a life-threatening iatrogenic complication of controlled ovarian hyperstimulation (COH) used in the treatment of infertility. OHSS is classified into four categories according to the severity of clinical findings and symptoms as mild, moderate, severe and critical. Although it is a fatal condition in the advanced stages, its pathogenesis is still not clearly understood. Therefore, this study aimed to define the organ damage that plays a role in the clinical course of OHSS and to evaluate the effects of OHSS severity on the kidney, liver, and lung both histomorphologically and histopathologically.

Methods: Our study employed 21 female immature wistar albino rats (22 day-old, weighing 30-40 g). The rats were randomly divided into three groups: the control group (n=7), moderate OHSS group (n=7) and severe OHSS group (n=7). The OHSS model was established with sequential injections of pregnant mare serum gonadotropin (PMSG) and human chorionic gonadotropin (hCG). Weight loss/gain (total body weight on the last day – total body weight on the first day) and organ weights of the rats were recorded. A routine tissue processing procedure was performed for the kidney, liver and lung fixed with formaldehyde. General histomorphological structures and damage evaluations of organs were made from sections stained with hematoxylin and eosin.

Results: In the intra-abdominal macroscopic evaluation, there was an increase in the size of the ovary, enlargement of the fallopian tubes and dilatation of the colon. The whole body and organ weights of the severe OHSS group were significantly higher than those of the control group ($p<0.01$). Statistically significant differences were noted in proximal tubule dilatation and increased necrosis in the kidney, sinusoidal and vascular congestion in the liver, degeneration in hepatocytes and in the scoring of lung damage ($p<0.01$).

Conclusion: Our study is the first to examine the histomorphological and histopathological effects of OHSS severity on the kidney, liver and lungs in rats. The data we obtained describe the organ damage caused by the severity of OHSS. Our findings can contribute to the elucidation of the pathogenesis of OHSS and the treatment process.

Keywords: Histomorphological evaluation, kidney, liver, lung, ovarian hyperstimulation syndrome.

Address for correspondence: Filiz Yılmaz, Hitit University, Erol Olçok Training and Research Hospital, Çepni Street, 19100, Çorum, Turkey.
Phone: +90 364 219 30 00 **E-mail:** drfilizyilmaz@gmail.com **ORCID:** 0000-0003-0505-3905
Received: 9 August 2022 **Revised:** 23 May 2023 **Accepted:** 28 May 2023 **Published:** 12 June 2023

INTRODUCTION

Ovarian hyperstimulation syndrome (OHSS) is a life-threatening iatrogenic complication of controlled ovarian hyperstimulation (COH) during assisted reproductive techniques (ART). OHSS is classified into four categories according to the severity of clinical findings and symptoms as mild, moderate, severe and critical. Mild OHSS cases are characterized by abdominal bloating and mild ascites, while there is ultrasound evidence of ascites, moderate abdominal pain, and nausea/vomiting in moderate OHSS cases. In severe OHSS cases, there are clinical ascites, oliguria, hematocrit values higher than 0.45, hyponatremia, hypo-osmolarity and hyperkalemia. Critical OHSS cases are characterized by tense abdomen, wide hydrothorax, hematocrit value higher than 0.55, thromboembolism and acute respiratory distress. In all in vitro fertilization (IVF) cycles, the incidence is 20-33% for mild OHSS, 3-6% for moderate OHSS, and 0.1-2% for severe and critical OHSS. The clinical manifestations of moderate, severe and life-threatening OHSS are believed to stem from increased vascular permeability due to the overproduction of vasoactive substances such as angiotensin and vascular endothelial growth factor (VEGF). Intravascular fluid moves into the interstitial spaces with these angiogenic factors and blood pressure decreases. This situation might be resulted in death due to ascites, pleural effusion, hypotension, multiorgan failure, oliguria following acute renal failure and thromboembolism. (1,2).

OHSS is a potentially fatal condition and its pathogenesis is not clearly understood. Today, researchers have been unable to prevent the development of OHSS, despite trying different treatments for the predicted pathogenesis to prevent OHSS. Therefore, further research is needed on the mechanisms causing OHSS or mediating the prevention of OHSS.

In the literature, the damage to internal organs caused by severe OHSS in humans has been evaluated with biochemical analyses (AST, ALT, GFR, creatinine), but the affected organs have not been evaluated histopathologically (3-6). Since animal experimental models are often preferred in the evaluation of diseases of unknown pathogenesis in humans, we have based our study on animal experimental models (7-11) representing OHSS severity classifications and aimed to examine the histomorphological and pathological effects of OHSS severity on the kidney, liver and lung.

MATERIALS AND METHODS

Experimental design

The experimental procedure of this study was approved by the Dokuz Eylül University Local Ethical Committee (Protocol No. 36/2021). The study was conducted in the Dokuz Eylül University Experimental Animals Laboratory in August 2021. It included 21 female immature wistar albino rats (22 days old, weighing 30-40 gr). Immature rats were used because they were compatible with similar studies in the literature and their previous cycles were not affected by the corpus luteum (7,12). During the experiment, the rats were kept in an environment where they could access water and food ad libidum at an average temperature of 22 °C, 20-40% humidity, 12 hours a day and 12 hours a night cycle.

The total body weight of the rats was measured on the first day and the last day of the experiment. The rats were randomly divided into three groups: control group (n=7), moderate OHSS group (n=7), and severe OHSS group (n=7). The control group was injected with 0.1 ml 0.9% sodium chloride (NaCl) i.p. for 6 consecutive days starting from the postnatal 22nd day. The moderate OHSS group was given 10 IU pregnant mare serum gonadotropin (PMSG). The PMSG was prepared in 0.1 ml 0.9% NaCl for 4 consecutive days starting from the postnatal 22nd day.Then, 10 IU and human chorionic gonadotropin (hCG) (i.p.) was prepared in 0.1 ml 0.9% NaCl on the 26th postnatal day (8,9). The severe OHSS group was given 10 IU PMSG prepared in 0.1 ml 0.9% NaCl for 4 consecutive days starting from the postnatal 22nd day and 30 IU hCG (i.p.) prepared in 0.1 ml 0.9% NaCl on the postnatal 26th day (7,8,9,12). All subjects were sacrificed on the postnatal 28th day (7-9,12). The abdomen was opened and model formation was evaluated macroscopically by qualitative methods such as ovarian size, the width of the fallopian tubes and colon morphology (13,14). Then, the lung, liver and kidney were excised. The weights of the removed organs were recorded and the organs were fixed in 4% formalin.

Histomorphological and histopathological examinations

Tissues fixed with formalin were embedded in paraffin 48 hours later and 5 micrometer thick sections were taken from these paraffin blocks. Hematoxylin and eosin (H&E) and periodic acid-schiff (PAS) staining protocols were applied. The histomorphological structures and general tissue properties of the organs were evaluated from sections stained with H&E. Ten preparations were selected from each group and 10 fields from each preparation

were photographed with an Olympus BX15 microscope (Olympus, Tokyo, Japan). Blind scoring was performed by a pathologist who did not know the group names and characteristics.

To assess the thickness of the epithelial and subepithelial smooth muscle layers of the bronchioles in the lung, four measurements were made in each airway at the 3, 6, 9 and 12 o'clock positions. Approximately 20 airways of each animal were evaluated, with two or three airways from each section.

Sections of the kidney were evaluated with PAS-stained preparations to easily distinguish between proximal and distal convoluted tubules. Morphometric analysis of renal corpuscles, glomeruli and proximal convoluted tubules (PCT) was performed from these sections (16). To randomize 10 renal corpuscles to be selected per animal, the area of the kidneys was chosen from their upper, middle and lower parts. For each group, 70 renal corpuscles and their associated glomeruli and 210 proximal convoluted tubules were analyzed at X400 magnification. The area, diameter, perimeter and radius were measured for both the renal body and the glomerulus. In addition, the area, perimeter, diameter, radius and lumen area of the three PCTs adjacent to the specific renal corpuscles to be evaluated were measured. The urinary space was calculated by subtracting the glomerular area from the renal corpuscle area. Measurements were made with the ImageJ software.

In the pathological evaluation of the kidney, inflammatory cells, necrosis, loss of cell structure, edema, granular appearance, vacuolization and fibrosis parameters were scored. Eckhoff's scoring and Suzuki scoring parameters were used for liver injury scoring (17-19). Kidney and liver scores were classified as absent (0), mild (1), or moderate (2) (20). The lung injury scoring system of the American Thoracic Society was used in the histopathological evaluation of the lung (21). At least 20 random regions were independently scored from 0 to 2.

Statistical analysis

The SPSS 24.0 software was used for analysis. All data were presented as the mean ± standard deviation. Histopathological evaluation scores were evaluated with Kruskal–Wallis and Mann–Whitney U tests (22). Subject body and organ weights and kidney morphological measurement comparisons were made using one-way ANOVA and post hoc Bonferroni test (23). P values less than 0.05 were considered statistically significant.

RESULTS

Macroscopic evaluation

In the intra-abdominal macroscopic evaluation, there was an increase in ovarian size, enlargement of the fallopian tubes and dilatation of the colon. Body weight and organ weight measurements on the last day were significantly higher in the severe OHSS group than in the control group. There was no significant difference between the moderate OHSS group and the control group (Figure 1).

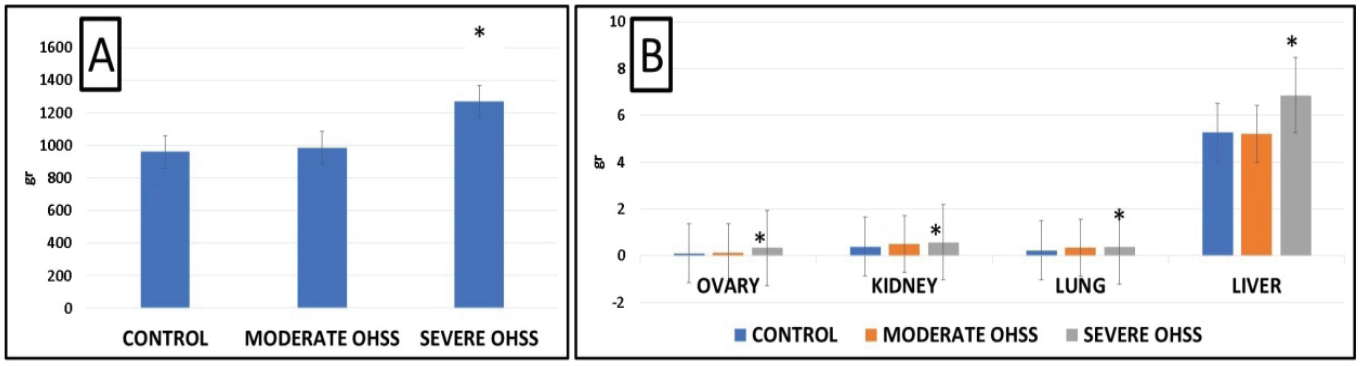

Figure 1. Body weight (**A**) and organ weight (**B**) measurements. (*p<0.01, severe OHSS group vs other groups).

Microscopic evaluation

Liver histomorphological and histopathological evaluation

Although liver index and liver function tests are important indicators to reflect the severity of liver damage, the gold standard is still histopathological examination. In the liver sections of the control group, sinusoids extending from the central veins and portal triad with normal histological structures were observed. Normal shape and healthy chromatin structure were detected in hepatocytes. There was no significant difference between the

control and moderate OHSS groups.

In the severe OHSS group, there were edema around the central vein, enlarged sinusoids, and dilatation in the portal triad structure. There was a significant difference between the severe and control and moderate OHSS groups ($p<0.01$). In addition, pyknosis, vacuolization and degeneration were significantly higher in hepatocytes, as evaluated by liver injury scoring. In severe OHSS, there were necrotic areas, hemorrhagic areas and mononuclear cell infiltration in some places (Figure 2).

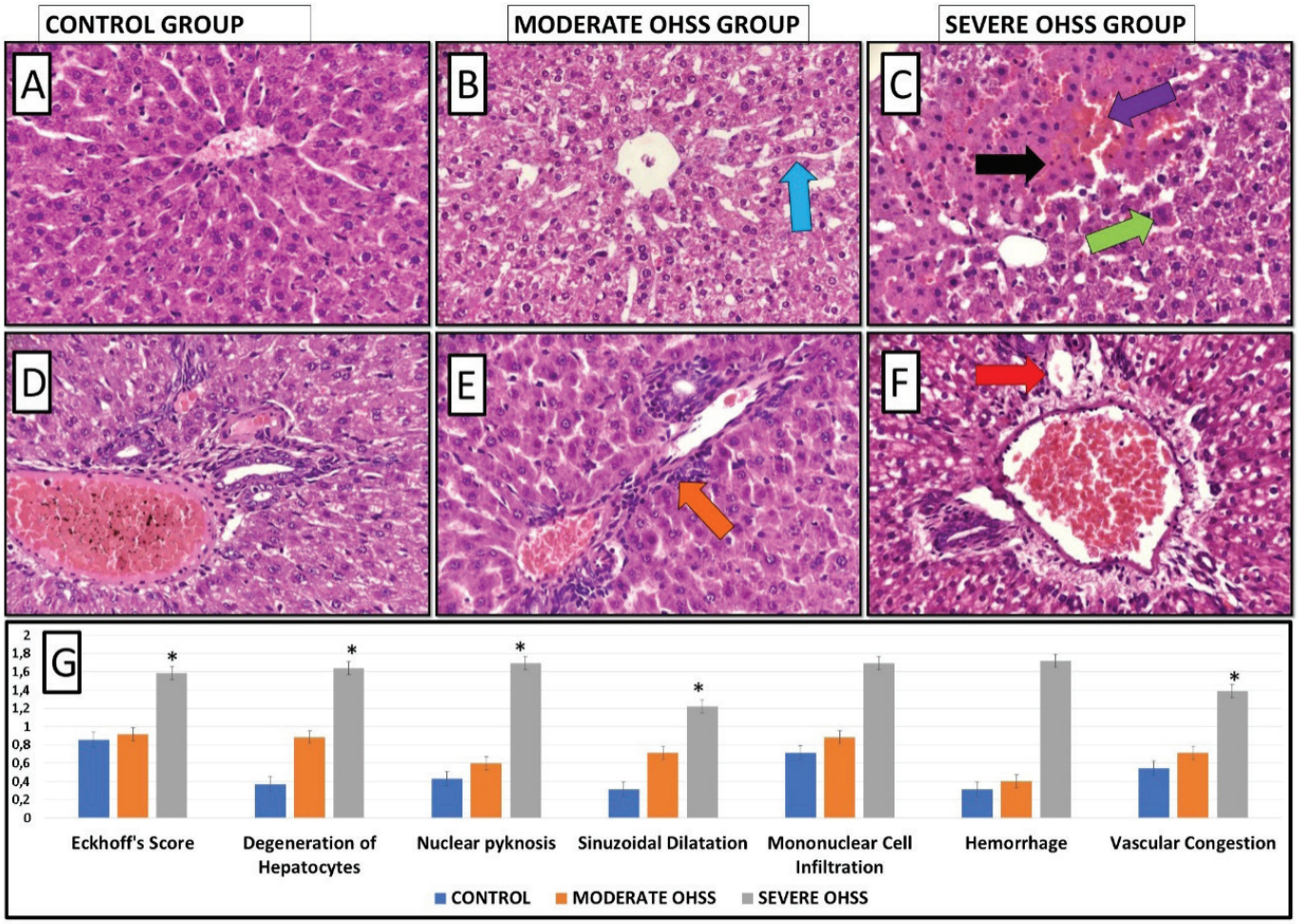

Figure 2. Light micrographs of rat liver tissue stained by H&E in the control (**A, D**) and OHSS groups (**B, C, E, F**) (40X), **G.** Scores of the histological changes in liver sections (Eckhoff's score, degeneration of hepatocytes, nuclear pyknosis, sinusoidal dilatation, mononuclear cell infiltration, vasculature congestion, hemorrhage). Black arrow; nuclear pyknosis, blue arrow; sinusoidal dilatation, red arrow; vascular congestion, green arrow; degeneration of hepatocytes, orange arrow; mononuclear cell infiltration, purple arrow; hemorrhage. (*$p<0.01$, severe OHSS group vs other groups).

Kidney histomorphological and histopathological evaluation

Vacuolization, pyknosis, dilatation, medullary congestion and Jablonski scoring necrosis parameters were scored in the histopathological evaluation of the kidney. For each parameter, the scores of the control group were significantly lower than those of the moderate and severe groups. There was no significant difference between the moderate and severe groups for vacuolization, dilatation and pyknosis parameters. There was a statistically significant difference between the moderate and severe groups for necrosis, Jablonski, cast formation, brush and medullar congestion parameters (Figure 3).

In the morphological evaluation of the kidney, area, perimeter and diameter measurements were performed for the renal corpuscle, glomeruli, proximal tubule and proximal tubule lumens. Renal corpuscle and glomeruli measurements were significantly lower in the control group than in the moderate and severe groups. There was no statistically significant difference between the moderate and severe groups. Proximal tubule measurements

were significantly lower in the control group than in the moderate and severe groups. There was no significant difference between the moderate and severe groups. The proximal tubule lumen measurements of the control group were significantly lower than those of the moderate and severe groups. There was also a significant difference between the moderate and severe groups. Urinary space measurements of the control group were significantly lower than those of the moderate and severe groups. There was no statistically significant difference between the moderate and severe groups (Figure 3).

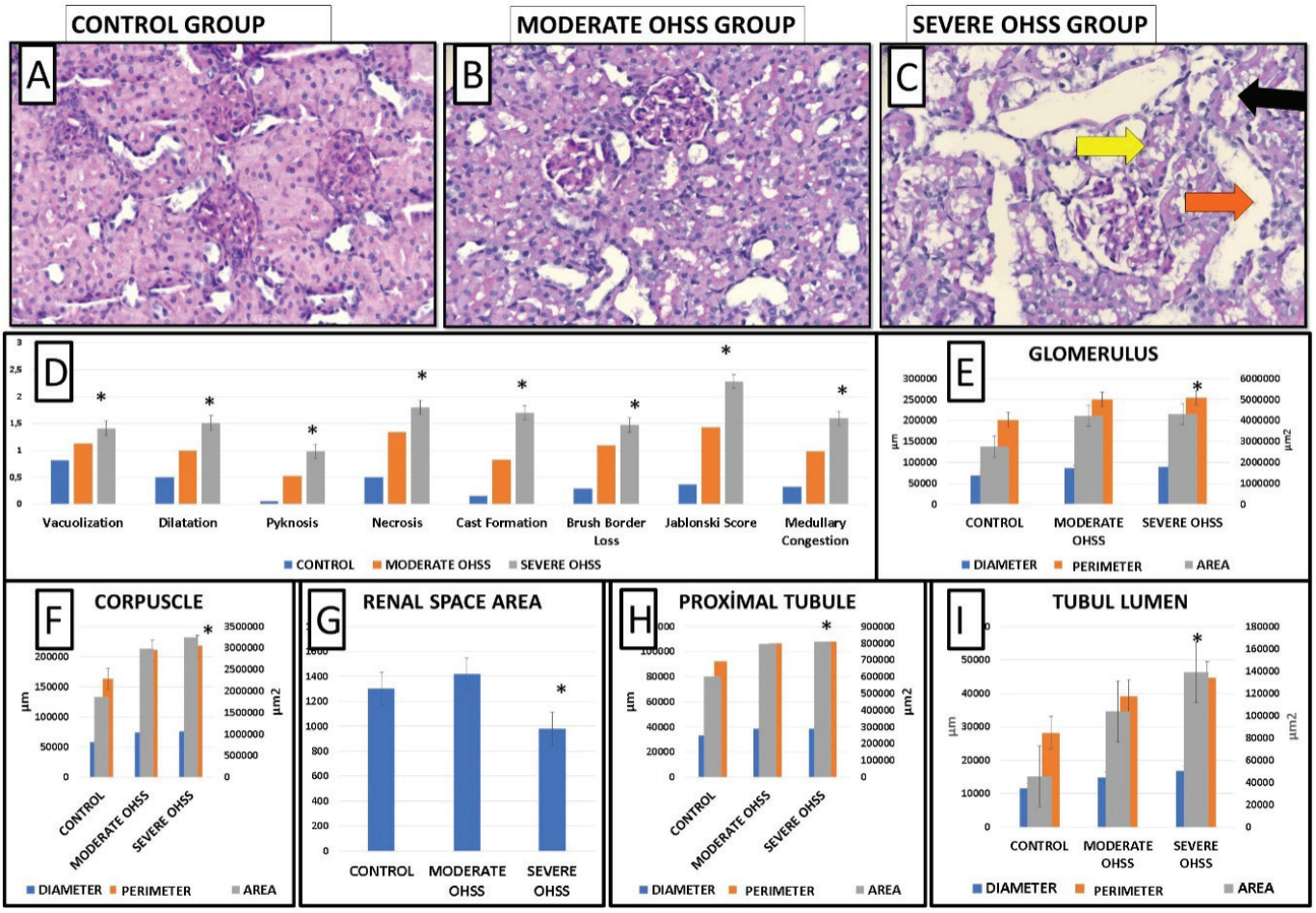

Figure 3. A. Light micrographs of rat renal tissue stained by PAS in the control (A) and OHSS groups (B-C) (40X). D) Renal injury scores (cellular vacuolization, tubular dilatation, nuclear pyknosis, necrosis, cast formation, brush border loss, Jablonski score, medullary congestion). The evaluation of area, perimeter, and diameter measurements of the glomerulus (E), renal corpuscle (F), renal space area (G), proximal tubule (H), and proximal tubule lumens (I). Black arrow; necrosis, yellow arrow; cellular vacuolization, orange arrow; tubular dilatation. (*p<0.01, Group severe OHSS group vs. other groups).

Lung histomorphological and histopathological evaluation

In the severe OHSS group, neutrophils in the alveolar and interstitial space, proteinaceous residues filling the air spaces and alveolar septal thickening parameters were statistically significant. Hyaline members were not observed in any of the three groups (Figure 4). Epithelial height and muscle layer thickness measurements of bronchioles were also significant (Figure 4).

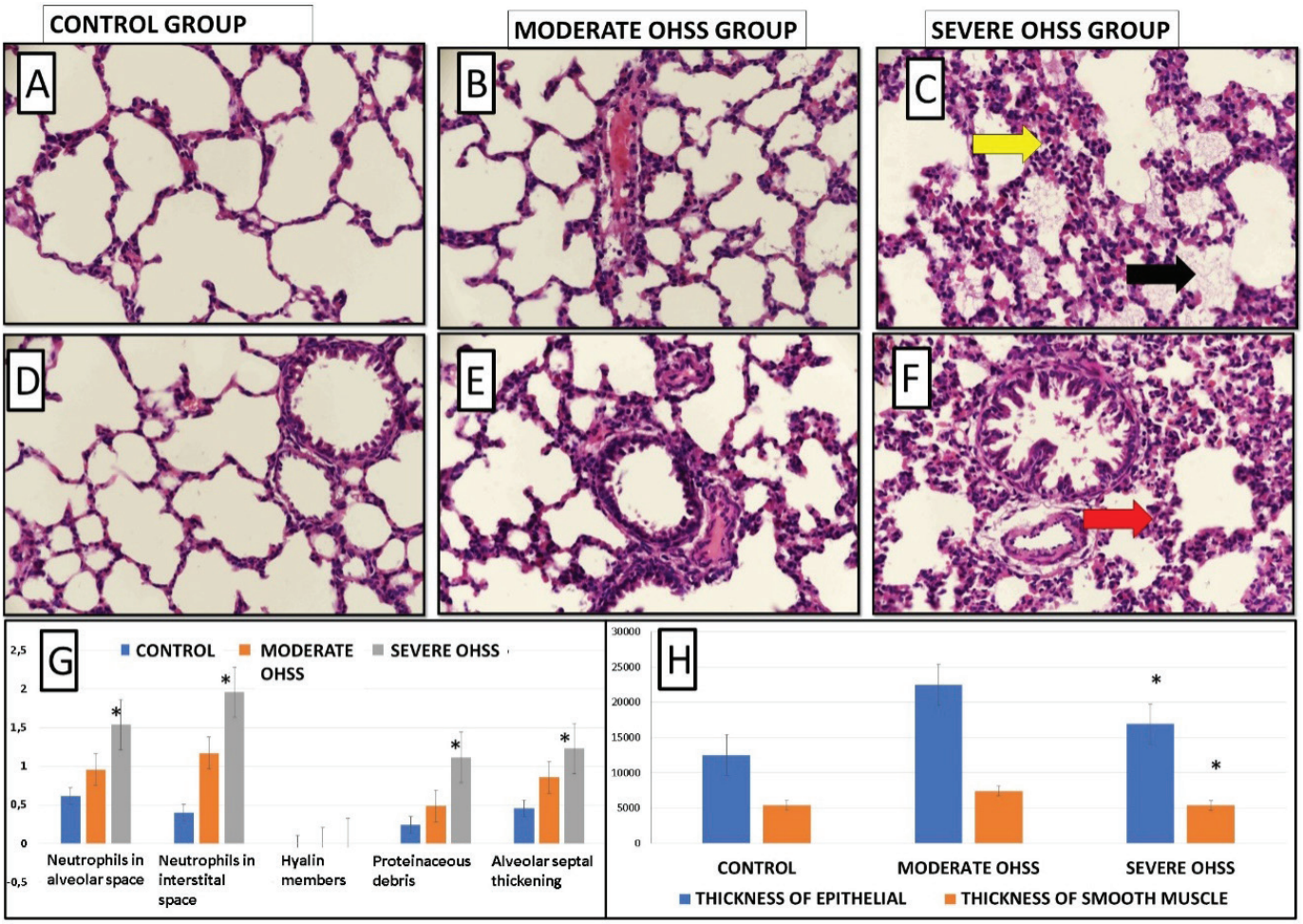

Figure 4. The effect of OHSS on lung histology (A-F) (40X, H&E), G. Lung injury scores (neutrophils in the alveolar space, neutrophils in the interstitial space, hyalin members, proteinaceous debris, alveolar septal thickening), H. Epithelial height and muscle layer thickness measurements of bronchioles. Black arrow; proteinaceous debris, yellow arrow; neutrophils in the interstitial space, red arrow; alveolar septal thickening. (*p<0.01, severe OHSS group vs.

DISCUSSION

COH is administered to patients to develop follicles during ART. The COH protocol or drug dose (normal, moderate or high) changes according to the clinical characteristics of the patient. OHSS is a life-threatening iatrogenic complication of COH. Depending on the severity of OHSS, clinical findings differ in patients. In advanced stages, it might be resulted in multiple organ failures (renal, hepatic, and respiratory dysfunction) and even death (1,2). This information led us to think that the severity of OHSS may differentially affect the histopathological findings of the organs. Therefore, we added moderate and severe OHSS groups to our study in addition to the control group. In the literature, Kasap et al. found that OHSS severity had a significant effect on body weight gain and ovarian weight in moderate and severe OHSS groups. This finding was interpreted as OHSS increasing fluid accumulation in the body, thus proving that they could create the OHSS model in rats (7). Similarly, we recorded body and organ weight gains in our macroscopic evaluation, particularly in the severe OHSS group, proving that we had successfully constructed our model.

Ohba et al. reported an increase in liver weight in the severe OHSS model but did not perform a histopathological evaluation of the organ (24). Similarly, we recorded the increase in liver weight and evaluated kidney and lung weights as well. We interpreted that the reason for the increase in liver weight was due to edema. In our study, the increase in liver, kidney and lung weights compared to the control group showed that these organs were also affected by the severity of OHSS.

In the literature, the effects of OHSS were evaluated histopathologically only in the ovary. However, our study aimed to evaluate organs beyond the ovary. Previous studies have evaluated the effect of OHSS on the kidneys through biochemical parameters (GFR, urea, creatinine) in humans and experimental animal models. Recent case reports have reported deteriorations in kidney, liver and lung function tests (25-27). During treatment, renal and liver function tests were observed to regenerate with strict fluid therapy monitoring and supplements such as human albumin solution to maintain intravascular volume (27).

In our study, tubular damage included vacuolization, pyknosis, brush border loss and cast formation in severe OHSS, whereas tubular damage was recorded as milder in moderate OHSS. The Jablonski scoring reflects the severity of proximal tubule necrosis. In severe OHSS, we observed histopathological findings to be consistent with acute renal failure, showing that tubular damage may play a role in the etiology.

Alteration of the glomerular structure can lead to decreased renal function due to its effects on tubular function. The increase in glomerular size can be attributed to compensation mechanisms. In our study, urinary space was significantly increased in the OHSS groups compared to the control group. This increase in the urinary space can be attributed to an increase in the renal corpuscle area or an increase in the glomerular area due to the deterioration of the cell architecture. The proximal tubule lumen increase may be attributes to the loss of the brush border of the proximal tubules, which would severely affect the reabsorption of essential molecules in the body. Although the effect of OHSS on tubular function has not been demonstrated in mice, our study has proved that it can cause tubular damage.

The literature has discussed hepatocellular dysfunction caused by severe OHSS with elevated serum AST and ALT. In our study, we supported this idea with our histopathological data. We microscopically evaluated portal vein and hepatic artery structures, the two main vessel structures providing blood supply to the liver. The presence of pathological edema in the vascular structures of the liver was remarkable. Similarly, dilatation was observed in the sinusoids opening to the hepatic artery, which can be attributed to edema in the vessels. We interpreted that VEGF and its associated vascular permeability increase, which are discussed most in the pathogenesis of OHSS, may be the underlying cause of edema in the vascular structures of the liver.

Hepatocytes are the basic cells of the liver that perform its function. If there is degeneration in hepatocytes, the loss of function is inevitable. The remarkable damage in hepatocytes in our study suggested that the damage may cause loss of organ function. In particular, necrotic areas in the liver can cause irreversible damage and accelerate death. Our results showed the presence of intense cytoplasmic vacuolization and moderately necrotic cell foci in the liver structure of rats with severe OHSS. Necrosis is characterized by organelle swelling with cell degeneration and shrinkage and dissolution of nuclei followed by amorphous cytoplasm. Cytoplasmic vacuolation refers to excessive lipid accumulation in cytoplasmic vesicles, but vacuolar formation has also been suggested as a cellular defense mechanism against toxic substances. Decomposing these substances in vacuoles may be a way to prevent them from interfering with cellular metabolism.

Limitations:

This study has some limitations. Its sample sizes are small. We limited animal mortality with fewer rats. We know it is challenging to evaluate the severity of OHSS based on animal studies only. More information may be obtained through further human research.

CONCLUSION

The damage observed in the OHSS might be resulted in multiorgan failure and death. Therefore, treatment planning is critical. In treatment planning, it is crucial to focus on symptom-oriented planning that will regress the etiology. Damage to organs plays a role in the emergence of symptoms. Therefore, our study aimed to histopathologically examine the effects of OHSS on the kidneys, liver and lungs depending on the severity. We believe that our data have helped to define the damage in organs and contributed to the elucidation of OHSS pathogenesis and the treatment process.

Acknowledgement: This research was presented as an oral presentation at 8th UTSAK Conference- VI, Ankara, 25–26 December 2021.
Conflicts of interest: All authors declare to have no conflict of interest.
Financial support and sponsorship: There is no funding of this study.
Ethical approval: The study was conducted with the conditions recommended by the Helsinki Declaration. The study was approved by the Dokuz Eylül University Local Ethical Committee (Protocol No. 36/2021).
Author contributions: All of the authors declare that they have all participated in the study, supervision, data collection&/or processing, performed data analysis, literature search, written, critical review.

References

1. Blumenfeld Z. The Ovarian Hyperstimulation Syndrome. Vitam Horm. 2018;107:423-51.
2. Practice Committee of the American Society for Reproductive Medicine. Electronic address: ASRM@asrm.org; Practice Committee of the American Society for Reproductive Medicine. Prevention and treatment of moderate and severe ovarian hyperstimulation syndrome: a guideline. Fertil Steril. 2016;106(7):1634-47.
3. Abou Arkoub R, Xiao CW, Claman P, Clark EG. Acute Kidney Injury Due to Ovarian Hyperstimulation Syndrome. Am J Kidney Dis. 2019;73(3):416-20.
4. Toftager M, Bogstad J, Bryndorf T, Løssl K, Roskær J, Holland T, et al. Risk of severe ovarian hyperstimulation syndrome in GnRH antagonist versus GnRH agonist protocol: RCT including 1050 first IVF/ICSI cycles. Hum Reprod. 2016;31(6):1253-64.
5. Khalil MA, Ghazni MS, Tan J, Naseer N, Khalil MA. Spontaneous Bacterial Peritonitis and Anasarca in a Female Patient with Ovarian Hyperstimulation Syndrome Complicated by Respiratory and Kidney Failure. Case Rep Gastroenterol. 2016;10(2):423-30.
6. Timmons D, Montrief T, Koyfman A, Long B. Ovarian hyperstimulation syndrome: A review for emergency clinicians. Am J Emerg Med. 2019;37(8):1577-84.
7. Kasap E, Turan GA, Eskicioğlu F, Cengiz H, Gur EB, Sivrikoz ON, et al. Comparison between resveratrol and cabergoline in preventing ovarian hyperstimulation syndrome in a rat model. Gynecol Endocrinol. 2016;32(8):634-40.
8. Ozgur S, Oktem M, Altinkaya SO, Oktem EO, Cenksoy C, Erdem O, et al. The effects of resveratrol on ovarian hyperstimulation syndrome in a rat model. Taiwan J Obstet Gynecol. 2018;57(3):383-8.
9. Zhang J, Huang J, He X, Li N, Miao Y, Li B, et al. Ginkgo biloba extract 761 reduces vascular permeability of the ovary and improves the symptom of ovarian hyperstimulation syndrome in a rat model. Gynecol Endocrinol. 2022;38(4):318-23.
10. Saylan A, Arioz DT, Koken T, Dilek H, Saylan F, Yilmazer M. Prevention of ovarian hyperstimulation syndrome in a rat model: efficacy comparison between cabergoline and meloxicam. Acta Obstet Gynecol Scand. 2010;89(5):692-99.
11. Bakırcı Ş, Sağsöz N, Devrim T, Şahin Y, Bulanık M, Gözüyukarı H. Effect of ondansetron for preventing of ovarian hyperstimulation syndrome: in an experimental rat model. Gynecol Endocrinol. 2022;38(12):1093-96.
12. Atilgan R, Pala Ş, Yavuzkır Ş, Başpınar M, Yılmaz M, Ilhan N. What is the impact of short- and long-term supplementation of either cabergoline or clarithromycin on resolving rat ovarian hyperstimulation syndrome (OHSS) model? J Obstet Gynaecol. 2019;39(5):687-94.
13. Turan GA, Eskicioglu F, Sivrikoz ON, Cengiz H, Adakan S, Gur EB, et al. Myo-inositol is a promising treatment for the prevention of ovarian hyperstimulation syndrome (OHSS): an animal study. Arch Gynecol Obstet. 2015;292(5):1163-71.
14. Darabi Z, Basir Z, Tabandeh MR, Ghotbeddin Z. Coenzyme Q10 improves ovarian histology and attenuates the expression of angiogenesis-associated proteins in the ovary of rats with experimental hyperstimulation syndrome. Iran J Basic Med Sci. 2022;25(8):989-96.
15. Ezzi L, Belhadj Salah I, Haouas Z, Sakly A, Grissa I, Chakroun S, et al. Histopathological and genotoxic effects of chlorpyrifos in rats. Environ Sci Pollut Res Int. 2016;23(5):4859-67.
16. Kotyk T, Dey N, Ashour AS, Balas-Timar D, Chakraborty S, Ashour AS, et al. Measurement of glomerulus diameter and Bowman's space width of renal albino rats. Comput Methods Programs Biomed. 2016;126:143-53.
17. Wen S, Li X, Ling Y, Chen S, Deng Q, Yang L, et al. HMGB1-associated necroptosis and Kupffer cells M1 polarization underlies remote liver injury induced by intestinal ischemia/reperfusion in rats. FASEB J. 2020;34(3):4384-402.
18. Jiang Y, Zeng Y, Huang X, Qin Y, Luo W, Xiang S, et al. Nur77 attenuates endothelin-1 expression via down regulation of NF-κB and p38 MAPK in A549 cells and in an ARDS rat model. Am J Physiol Lung Cell Mol Physiol. 2016;311(6):L1023-L1035.
19. Shi B, Wang XQ, Duan WD, Tan GD, Gao HJ, Pan YW, et al. Effects of positive acceleration (+Gz stress) on liver enzymes, energy metabolism, and liver histology in rats. World J Gastroenterol. 2019;25(3):346-55.
20. Truter D, Chellan N, Strijdom H, Webster I, Rawstorne J, Kotzé SH. Histomorphological changes in the pancreas and kidney and histopathological changes in the liver in male Wistar rats on antiretroviral therapy and melatonin treatment. Acta Histochem. 2018;120(4):347-55.
21. Song LC, Chen XX, Meng JG, Hu M, Huan JB, Wu J, et al. Effects of different corticosteroid doses and durations on smoke inhalation-induced acute lung injury and

pulmonary fibrosis in the rat. Int Immunopharmacol. 2019;71:392-403.

22. Koca U, Olguner ÇG, Ergür BU, Altekin E, Taşdöğen A, Duru S, et al. The effects of dexmedetomidine on secondary acute lung and kidney injuries in the rat model of intra-abdominal sepsis. Scientific World Journal. 2013;2013:292687.

23. Işık S, Uzuner N, Karaman M, Karaman Ö, Kıray M, Kozanoğlu İ, et al. Effects of Intraperitoneal Injection of Allogeneic Bone Marrow-derived Mesenchymal Stem Cells on Bronchiolitis Obliterans in Mice Model. Iran J Allergy Asthma Immunol. 2017;16(3):205-18.

24. Ohba T, Ujioka T, Ishikawa K, Tanaka N, Okamura H. Ovarian hyperstimulation syndrome-model rats; the manifestation and clinical implication. Mol Cell Endocrinol. 2003;202(1-2):47-52.

25. Ma XW, Yin JW, Yang R, Yang S, Li J, Wang Y, et al. Clinical characteristics of severe late-onset ovarian hyperstimulation syndrome and its impact on the live birth outcome of IVF-ET. Zhonghua Fu Chan Ke Za Zhia. 2022;57(9):678-85.

26. Tsangaris I, Paramythiotou E, Tsaknis G, Argentos S, Antoniadou A, Kopterides P, et al. Ovarian hyperstimulation syndrome complicated by severe community-acquired pneumonia due to methicillin-resistant Staphylococcus aureus positive for Panton-Valentine leukocidin. J Obstet Gynaecol Res. 2012;38(2):476-8.

27. Kasaven LS, Goumenou A, Adegoke K. Multiorgan failure associated with severe ovarian hyperstimulation syndrome due to inadequate protocol optimisation: a rare but avoidable complication. BMJ Case Rep. 2018;2018:bcr2017223418.